JOURNAL OF MATERIALS SCIENCE 22 (1987) 2203–2208

High-field electrical conduction in HgI_2

M. M. ABDUL-GADER, K. A. WISHAH, Y. A. MAHMUD,
R. N. AHMAD-BITAR
Department of Physics, University of Jordan, Amman, Jordan

The electrical and dielectric properties of illuminated HgI_2 were studied at room temperature under various a.c.-signal amplitudes in the frequency range 1 Hz to 10 kHz. Below 40 Hz, the real part of the dielectric constant, ε', was found to vary slightly with voltage for low electric fields ($E < 10^3\,\mathrm{V\,cm^{-1}}$), above which it showed a steady increase with the applied voltage. At higher frequencies, no voltage dependence of ε' (or the geometrical capacitance) of the crystal was observed. On the other hand, the imaginary part of the dielectric constant, ε'', or the a.c. conductivity, σ ($=\omega\varepsilon_0\varepsilon''$) was found to decrease considerably with the applied voltage for $E < 10^3\,\mathrm{V\,cm^{-1}}$ at all frequencies. For higher fields ($E > 10^3\,\mathrm{V\,cm^{-1}}$), $\sigma \propto \exp\,[C(E/\varepsilon')^{1/2}]$, where C is a constant. Above 40 Hz, this variation was in good agreement with the behaviour of the bulk resistance of the crystal. Such behaviour is discussed in the view of Richardson–Schottky and Poole–Frenkel conduction mechanisms, which seem to be operative in HgI_2 at room temperature.

1. Introduction

Mercuric iodide (HgI_2) is a promising material for low-energy γ-ray and X-ray detectors at room temperature [1–9]. It is an insulator with an energy-band gap of 2.13 eV and a dark resistivity of the order of $10^{13}\,\Omega\,\mathrm{cm}$. Even for the high-purity HgI_2 crystals, the hole mobility at room temperature is low ($\mu \sim 4\,\mathrm{cm^2\,V^{-1}\,sec^{-1}}$). Therefore, a thin HgI_2 detector crystal is necessary to have efficient charge collection and to overcome polarization effects [7–12]. This, in turn, puts a restriction on the voltage applied to the HgI_2 crystal. Moreover, the presence of impurities and defects in the crystal would introduce various trapping and impurity levels throughout the insulator, leading to incomplete charge collection and deterioration of the detector efficiency. Their presence will increase the dielectric constant of the material, and hence the detector capacity. In addition, these impurities and defects lead to a decrease in the inherent resistivity of the crystal and thus increase the leakage current. These two aspects are responsible for the noise contribution and this would give a low signal-to-noise ratio in the detector.

Therefore, it is of great importance to study the conduction process in HgI_2 crystals and their dielectric properties under various experimental conditions such as frequency, temperature, voltage, illumination [13–18]. Various conduction mechanisms [19] such as tunnelling, Richardson–Schottky, Poole–Frenkel effects, thermal ionization of traps and impurities and space charge-limited conduction may be invoked to explain the electrical transport phenomena in materials [20–27]. The tunnelling effect is best observed in extremely thin insulators (~ 3 nm thick), but it is the thicker insulators in which the Poole–Frenkel and Schottky effects apparently manifest themselves, in particular at high temperatures and in high electric fields. Space charge-limited currents depend on the applied voltage, thickness and the temperature. It has been found experimentally and theoretically that these effects are greatly enhanced by the application of electric field to the crystal [20–27], giving rise to more conduction charge carriers and hence lowering the electrical resistivity of the material. Consequently, the dependence of the dielectric constant, loss and conductivity of HgI_2 on the applied voltage will be of great interest. A study of this type has been undertaken in the present work on an illuminated HgI_2 crystal of about 20 μm thickness at room temperature and as function of frequency and peak-to-peak voltage of the applied a.c. signal. This study would lead to a better understanding of the possible conduction mechanisms that occur in the HgI_2 material. Moreover, such a study might give an idea about the maximum operating voltage of the detector, which obviously depends on the thickness of its crystal.

2. Experimental details

The HgI_2 cell (crystal plus contacts) used in the present study is the one used in our previous work [11, 17, 18]. The crystal was kept under constant intensity of light from a yellow LED placed at about 1 cm above the crystal. Measurement of impedance and phase angle as a function of frequency (1 Hz to 10 kHz) were made for several values of peak-to-peak voltage, V_{pp}, of the a.c. signal applied to the cell. The values of V_{pp} lie in the range 0.5 to 12 V, corresponding to an electric field as high as $2 \times 10^3\,\mathrm{V\,cm^{-1}}$. The accuracy in the measured values of impedance and phase angle was better than 5% [13]. The electrical circuit and experimental procedure for measuring the impedance and phase angle produced by the HgI_2 cell were described elsewhere [11, 28]. The electrical parameters of the cell under study as well as the real and imaginary part of its dielectric constant, and hence its a.c. conductivity,

0022–2461/87 $03.00 + .12 © 1987 Chapman and Hall Ltd.

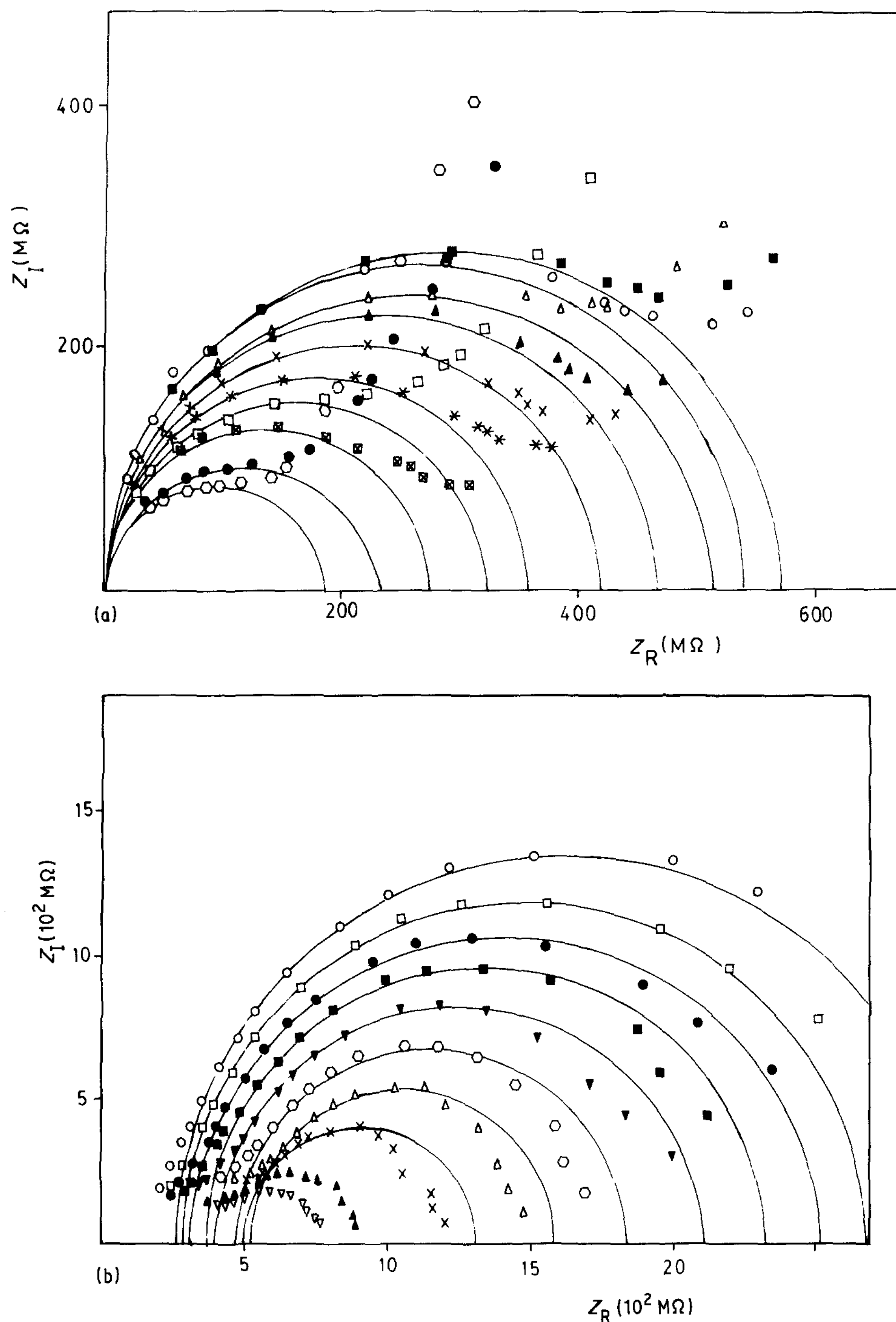

Figure 1 Complex impedance plane plot for an illuminated HgI_2 cell under various peak-to-peak voltages for (a) $f > 40$ Hz; (b) $f < 40$ Hz. (a) ⊠ 0.5 V, * 1 V, × 1.5 V, ▲ 2 V, ○ 3 V, ■ 4 V, △ 5 V, □ 7 V, ● 9 V, ⬡ 10 V. (b) ○ 10 V, □ 9 V, ● 8 V, ■ 7 V, ▼ 6 V, ⬡ 5 V, △ 4 V, × 3 V, ▲ 2 V, ▽ 1.5 V.

were then extracted from these measurements as discussed previously [11, 13, 29].

3. Results and discussion

Fig. 1a shows the complex impedance plane plots [30] in the high frequency region ($f > 40$ Hz) for different values of the peak-to-peak voltage, V_{pp}, of the a.c. signal applied to an illuminated HgI_2 cell. The corresponding plots at lower frequencies are shown in Fig. 1b. Obviously, the electrical characteristic of the HgI_2 cell changes drastically with the applied voltage. The data were analysed on the basis of an electrical equivalent network that was supposed to represent the HgI_2 cell [11, 13]. In the high frequency region, such analysis showed that the bulk capacitance, C_b, of the sample has a value of about 2 pF and is almost independent of the applied a.c. voltage in the range studied. It is worth-noting that C_b of high-quality HgI_2 crystals does not also depend on temperature in the range $100\,K < T < 300\,K$ [14, 17] and the intensity or the wavelength of light [29]. The bulk resistance, R_b, of the sample was found to increase considerably with increasing voltage up to $V_{pp} \sim 4$ V, corresponding to an electric field of about $10^3\,V\,cm^{-1}$, beyond which it starts to decrease steeply with further increase in the applied a.c. voltage as shown in Fig. 2. The bulk resistance was found to follow an exponential dependence on V_{pp} of the form $R_b \propto \exp\,[A(V_{pp})^{1/2}]$ with slope, A, ~ 0.7 for $V_{pp} < 4$ V and of about -1 at higher voltages.

In the low frequency region ($4\,Hz < f < 40\,Hz$), the analysis of the appropriate complex impedance plots at various values of V_{pp} showed that the corresponding capacitance of the cell does depend on the applied voltage. The activation resistance, R_a, of the cell [11] increases monotonically with increasing V_{pp} over the whole range studied as seen in Fig. 2.

The nature of variation of a.c. electrical and dielectric

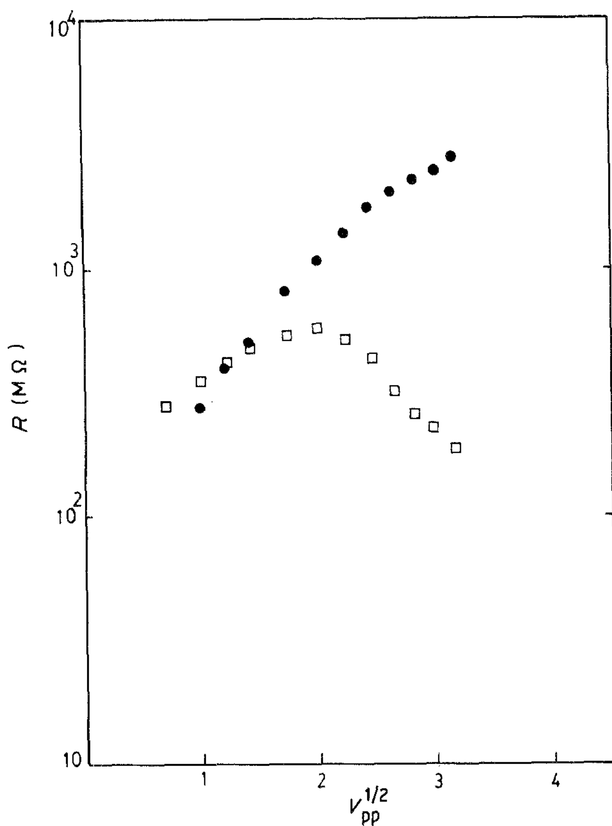

Figure 2 Voltage-dependence of the bulk resistance, R_b (□), and activation resistance, R_a (●), of the HgI_2 cell [11].

parameters of a solid with frequency could yield valuable information about the various polarization and conduction mechanisms present in the sample under investigation. These parameters can be either measured directly [12–14, 16, 22] or obtained from the measured values of the complex impedance, Z, and phase angle, ϕ, produced by the cell being studied [29]. The dielectric loss of a material is usually characterized by the dielectric loss angle, δ, which is given by

$$\tan\delta = \varepsilon''/\varepsilon' = \cot\phi \qquad (1)$$

where ε' and ε'' are, respectively, the real and imaginary parts of the complex dielectric constant, ε^*, of the material [$\varepsilon^* = \varepsilon' - j\varepsilon''; j = (-1)^{1/2}$]. In the terms of the complex impedance of the sample, ε^* is expressed by

$$Z = 1/j\omega C_0\varepsilon^* = Z_R - jZ_I \qquad (2)$$

where $\omega = 2\pi f$ is the angular frequency of the a.c. signal, C_0 is the geometrical capacitance of the empty condenser, and Z_R and Z_I are, respectively, the real and imaginary parts of the complex impedance. The a.c. conductivity of the material is related to the above dielectric parameters as

$$\sigma = \omega\varepsilon_0\varepsilon' \tan\delta = \omega\varepsilon_0\varepsilon'' \qquad (3)$$

where ε_0 is the permitivity of free space. The above equations were used to find ε', ε'', $\tan\delta$ and σ of our HgI_2 sample. Figs 3a to d show the room-temperature behaviour of these a.c. parameters with frequency at various peak to peak voltages. It is clear that the dielectric loss tangent, $\tan\delta$, varies appreciably with frequency and applied a.c. voltage; its actual behaviour varies from one region of frequency or voltage to another and depends on the corresponding behaviour of both ε' and ε''. The real part of the dielectric constant, ε', is voltage dependent and has larger values at low frequencies (< 40 Hz). Above 40 Hz, it decreases with increasing frequency, attaining a constant value for all applied voltages ($\varepsilon' \sim 5$, corresponding to a capacitance of 2 pF for our HgI_2 crystal as previously found). This behaviour of ε' at low frequencies may be attributed to space charge and/or dipolar polarization. The imaginary part of the dielectric constant, ε'', decreases linearly with $1/f$ at low voltages so that the conductivity, σ, is almost independent of frequency (see Fig. 3d). Nevertheless, the behaviour of ε'' with frequency changes as the voltage increases in a manner such that $\varepsilon'' \propto 1/f$ for $f < 10$ and > 100 Hz. However, it tends to become less dependent on frequency in the region 10 to 10^2 Hz at high voltages; thereby yielding a frequency-dependent conductivity in this region. The observed behaviour of $\tan\delta$ and ε'' (or σ) with frequency clearly show that there is a distinct relaxation phenomenon, being pronounced at high voltages, with a relaxation time determined by

$$\tau = 1/\omega\tan\delta = \varepsilon_0\varepsilon'/\sigma \qquad (4)$$

which corresponds roundly to 10 to 10^2 Hz. In this region, the plot of σ against f indicates that the a.c. conductivity $\sigma(\omega)$, of the illuminated HgI_2 sample varies with frequency as $\sigma(\omega) \propto \omega^s$, where the exponent s increases with peak-to-peak voltage. The frequency dependence of conductivity in solids might be attributed to hopping conduction or other sources of dielectric loss mechanisms [31, 32]. This frequency-behaviour of a.c. conductivity will be discussed in more detail in an additional publication.

The nature of the variation of a.c. properties of HgI_2 with the applied peak-to-peak voltage, V_{pp}, is largely changed as the voltage increases as clearly seen in Figs 4a to c. At low frequencies, the behaviour of both ε' and ε'' with V_{pp} gives us the dependence of the loss tangent, $\tan\delta$, on V_{pp}. However, the variation of $\tan\delta$ with V_{pp} in the high-frequency region becomes entirely due to ε'' as the high-frequency ε' is almost constant over the whole voltage region studied (see Fig. 4a). Only in the low frequency region does ε' vary with V_{pp}; it decreases slowly with increasing a.c. voltage up to $V_{pp} \sim 4$ V and then starts to increase considerably with further increase in the peak-to-peak voltage. On the other hand, the imaginary part of the dielectric constant, ε', exhibits a remarkable variation with the applied voltage at all frequencies. In the low-voltage region ($V_{pp} < 4$ V), ε' decreases considerably with increasing V_{pp} at any frequency, whereas in the high-voltage region it shows a decrease with an increase in V_{pp} for $f < 40$ Hz and then becomes an increasingly strong function of V_{pp} at higher frequencies.

The slow decrease of ε' with the applied voltage (< 4 V) observed at low frequencies (< 40 Hz) is thought to be due to a decrease in the space charge polarization. This type of polarization is dominant at low frequencies but decreases appreciably with increasing frequency and thus it contributes negligibly to ε' at high frequencies. On the other hand, the remarkable variation of $\varepsilon''(\propto\sigma)$ of the HgI_2 sample

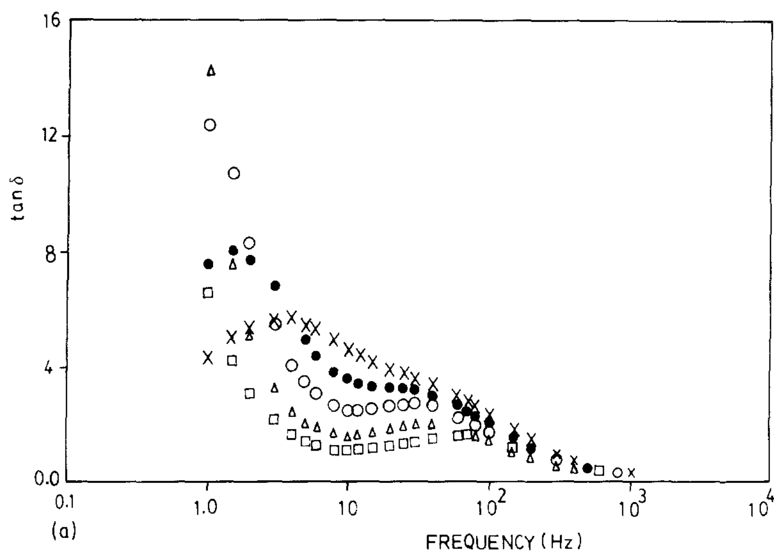

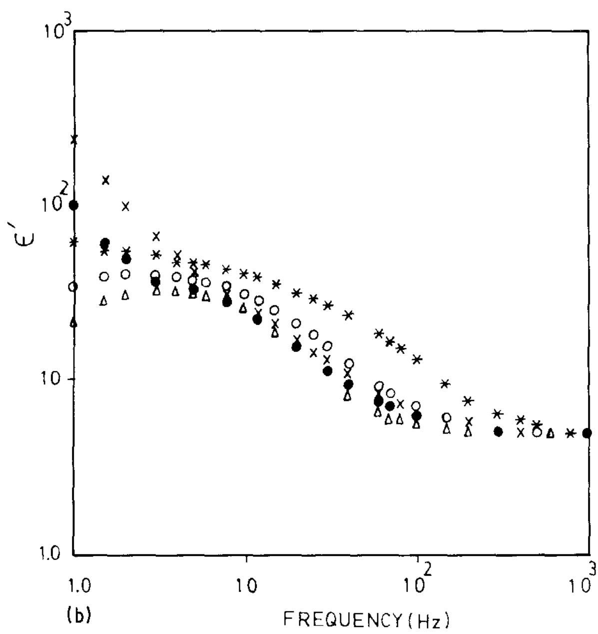

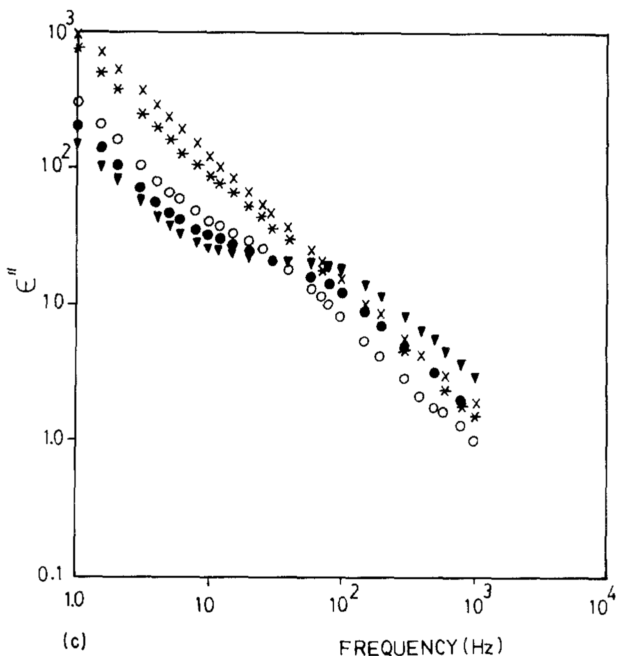

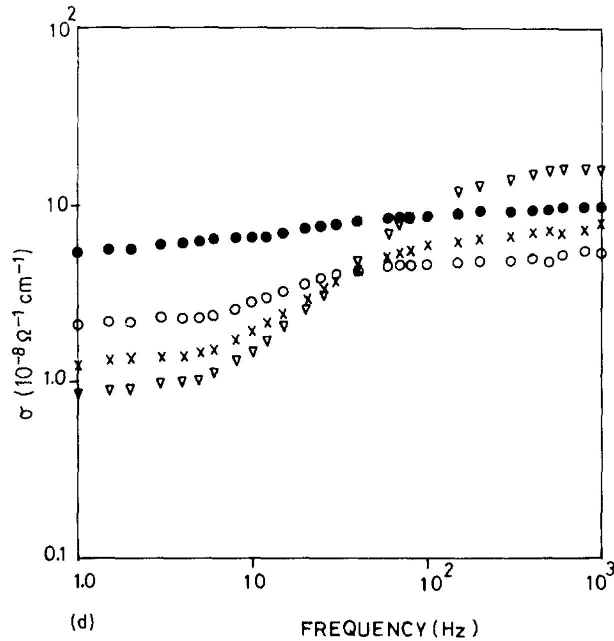

Figure 3 Variation of (a) tan δ, (b) ε', (c) ε'', and (d) σ of the HgI_2 cell with frequency under different peak-to-peak voltages. (a) × 0.5 V, ● 1.0 V, ○ 2.0 V, △ 4.0 V, □ 6.0 V. (b) × 0.5 V, ● 1 V, △ 4 V, ○ 6 V, ∗ 10 V. (c) × 0.5 V, ∗ 1 V, ○ 4 V, ● 7 V, ▼ 10 V. (d) ● 0.5 V, ○ 3 V, × 6 V, ▽ 10 V.

with the applied a.c. signal ($V_{pp} < 4$ V) seems quite interesting because all the graphs shown in Fig. 3a are nearly straight lines having about the same slope (~ 0.6) at all frequencies. These results are in fair agreement with the voltage-dependence of the bulk resistor, $R_b(\propto 1/\sigma)$, shown in Fig. 2. In this low-voltage region, the observed behaviour of ε' (or σ) with the applied a.c. voltage is not fully understood. However, one may not exclude the possibility of dissipation of charge carriers by a certain dielectric loss mechanism and/or the charged-carrier mobility seems to decrease with the applied electric field.

The voltage-behaviour of ε'' observed in the high-voltage region ($V_{pp} > 4$ V) is apparently due to some conduction mechanisms that become dominant at high electric fields, such as Richardson–Schottky (RS) and/or Pool–Frenkel (PF) effects [19–27]. The former effect is a field-assisted thermoionic emission due to the injection of charge carriers from the electrodes into the conduction band of the dielectric over a potential barrier, the height of which is field dependent. In the Poole–Frenkel effect, the current flowing in an insulator is considered to be due to the field

assisted thermal excitation of carriers from traps into the conduction band of the material. Both of these effects give the conductivity, σ, or ε'' ($= \sigma/\omega\varepsilon_0$) a field dependence of the form [19–27]

(Poole–Frenkel)

$$\sigma = \sigma_0 \exp [\beta_{PF} E^{1/2}/\theta k_B T] \quad (5)$$

(Richardson–Schottky)

$$\sigma = \sigma_0 \exp [\beta_{RS} (\alpha E)^{1/2}/k_B T] \quad (6)$$

where σ_0 is the low-field conductivity of the system, $\beta_{PF} = (e^3/\pi\varepsilon_0\varepsilon')^{1/2}$ and $\beta_{RS} = (e^3/4\pi\varepsilon_0\varepsilon')^{1/2}$, E is the electric field strength in the insulator ($= V/d$, where V is the applied voltage and d is the crystal thickness), e is the electronic charge, T is the absolute temperature and k_B is Boltzmann's constant. The parameter θ in Equation 5 ranges from 1 to 2 depending on the position of the Fermi level [24, 26], while the factor α of Equation 6 expresses the increase of the field at the electrodes over the charge-free value due to accumulation of space charge inside the material and at the boundaries.

Fig. 4b suggests that Richardson–Schottky and/or Poole–Frenkel conduction mechanisms are probably operative in HgI_2 material in the presence of high electric field as the functional dependence of the conductivity σ ($= \omega\varepsilon_0\varepsilon''$) upon field is almost the same for both effects. One can differentiate readily between the two types of conduction mechanisms from the behaviour of the conductivity with the applied electric field, a plot of $\ln \sigma$ against $V_{pp}^{1/2}$ results in a straight line of slope involving β_{RS} or β_{PF}. These experimentally determined factors can be compared with the theoretical values of β_{RS} and β_{PF}, which can be calculated accurately provided that the high-frequency dielectric constant of the material is known. In the high-voltage region, our results clearly show that the plots of $\ln \varepsilon''$ against $V_{pp}^{1/2}$ (Fig. 4b) are straight lines only at high frequencies ($f > 40$ Hz). At lower frequencies, ε' increases appreciably with increasing V_{pp} and is apparently the dominant factor in Equations 5 and 6 through Richardson–Schottky and Poole–Frenkel constants, namely β_{RS} and β_{PF}. This explains the observed decrease of ε'' (or σ) with V_{pp} below 40 Hz. However, at higher frequencies, ε' tends to become constant at all voltages (see Fig. 4a) and thus the conductivity starts to increase with the applied voltage in accordance with Equation 5 and/or 6. The graphs of $\ln \varepsilon''$ against $V_{pp}^{1/2}$ at $f > 40$ Hz and $V_{pp} > 4$ V (Fig. 4b) show that these are straight lines with a slope of about unity, in excellent agreement with the observed behaviour of R_b with V_{pp} (Fig. 2).

Detailed analysis of our results showed that the experimentally determined slopes of the graphs of

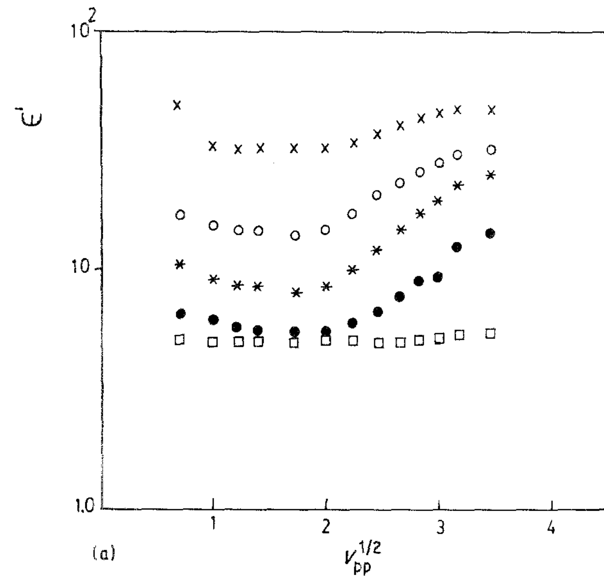

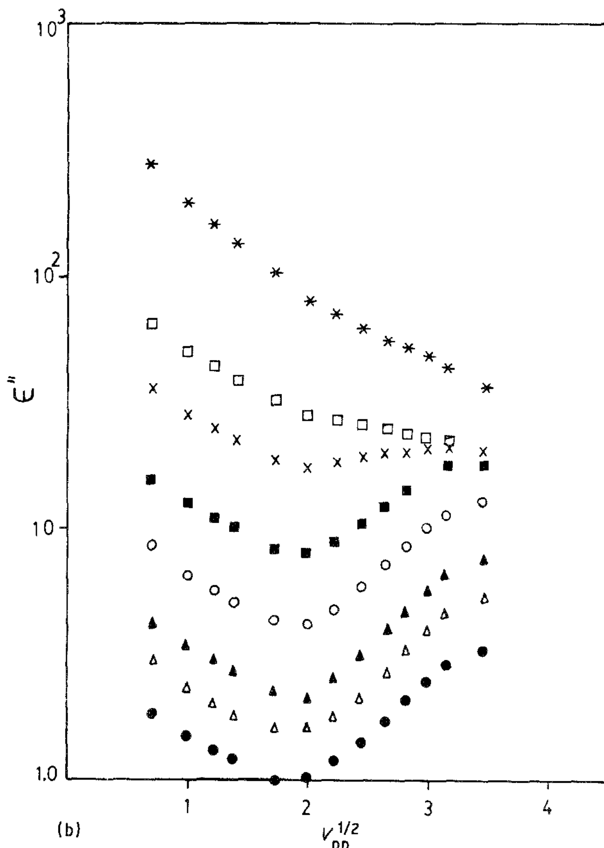

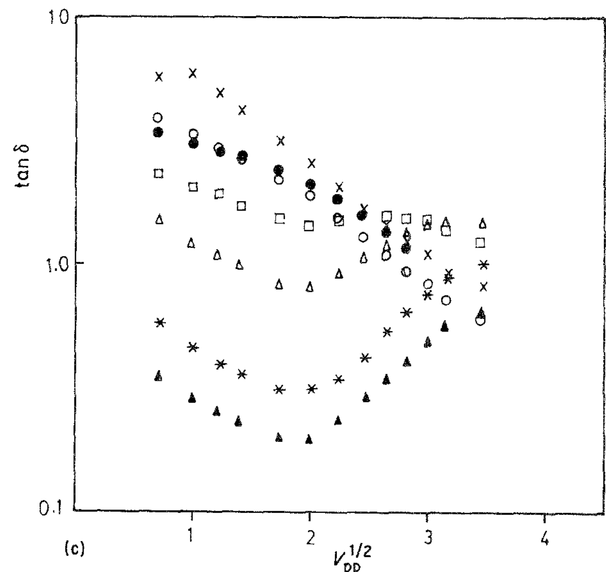

Figure 4 Voltage-dependence of (a) ε', (b) ε'', and (c) $\tan \delta$ of the HgI_2 cell for various frequencies. (a) × 4 Hz, ○ 20 Hz, * 40 Hz, ● 100 Hz, □ 600 Hz. (b) * 4 Hz, □ 20 Hz, × 40 Hz, ■ 100 Hz, ○ 200 Hz, ▲ 400 Hz, △ 600 Hz, ● 1000 Hz. (c) × 4 Hz, ○ 20 Hz, ● 40 Hz, □ 100 Hz, △ 200 Hz, * 600 Hz, ▲ 1000 Hz.

ln ε'' against $V_{pp}^{1/2}$ (Fig. 4b) are an order of magnitude larger than that obtained theoretically for Richardson–Schottky effect (Equation 6 with $\alpha = 1$ and $T = 300$ K). On the other hand, it is a factor of 5 greater than that found for Poole–Frenkel effect (Equation 5 with $\theta = 1$ and $T = 300$ K). This does not allow any definite conclusion for determining the actual conduction mechanism operative in HgI_2 material. Hence it may be concluded that perhaps both the mechanisms, i.e. the Richardson–Schottky and the Poole–Frenkel, are operative simultaneously in HgI_2 at room temperature.

References

1. A. J. DABROWSKI and G. C. HUTH, *IEEE Trans. Nucl. Sci.* **NS-25** (1978) 205.
2. A. J. DABROWSKI, G. C. HUTH, M. SINGH, T. E. ECONOMOU and A. L. TURKEVICH, *Appl. Phys. Lett.* **33** (1978) 211.
3. A. J. DABROWSKI, J. S. IWANCZYK, J. B. BARTON, G. C. HUTH, R. WHITED, C. ORTALE, T. E. ECONOMOU and A. L. TURKEVICH, *IEEE Trans. Nucl. Sci.* **NS-28** (1981) 536.
4. M. SLAPA, G. C. HUTH, W. SEIFT, M. SCHIEBER and P. RANDTKE, *ibid.* **NS-23** (1976) 102.
5. S. SWIORKOWSKI, G. ARMANTROUT and R. WICHNER, *IEEE Trans. Nucl. Sci.* **NS-21** (1974) 302.
6. P. A. TOVE, *Sens. Actuators* (*Switz.*) **105** (1984) 203.
7. A. FRIANT, J. MELLET, C. SALIOU and T. MOHAMMED BRAHIM, *IEEE Trans. Nucl. Sci.* **NS-27** (1980) 281.
8. T. MOHAMMED-BRAHIM, A. FRIANT and J. MELLET, *Phys. Status Solidi (a)* **79** (1983) 71.
9. W. SEIFT, M. SLAPA and G. C. HUTH, *Nucl. Inst. Meth.* **135** (1976) 573.
10. M. M. HASSAN, RIYAD N. AHMAD-BITAR, Y. MAHMOUD and K. WISHAH, *Egypt. J. Solids* **7** (1985) 113.
11. R. N. AHMAD-BITAR, M. M. ABDUL-GADER, K A. WISHAH, Y. A. MAHMOUD and M. A. HASSAN, *Nucl. Inst. Res. Meth. Phys.* **A243** (1986) 505.
12. M. RAMA RAO, D. ROY and J. K. D. VERMA, *J. Phys. D.* **18** (1985) 517.
13. J. L. REGOLINI and J. J. SAURA, *Appl. Phys.* **54** (1983) 1528.
14. P. SURYANARAYANA, H. N. ACHARYA and K. V. RAO, *J. Mater. Sci. Lett.* **3** (1984) 21.
15. C. DE BLASI, S. GALUSSIN, C. MANFREDOTTI, G. MICOCCI, L. RUGGIERO and A. TEPORE, *Nucl. Inst. Meth.* **150** (1978) 103.
16. D. P. YADAV, K. V. RAO and H. N. ACHARYA, *Phys. Status Solidi (a)* **60** (1980) 273.
17. R. N. AHMAD-BITAR, Y. A. MAHMUD, K. A. WISHAH, M. M. ABDUL-GADER and M. AL-HAJ ABDALLAH, *Egypt. J. Solids* **8** (1986) in press.
18. Y. A. MAHMUD, K. A. WISHAH, M. M. ABDUL-GADER, M. AL-HAJ ABDALLAH and R. N. AHMAD-BITAR, *Appl. Phys. A* **41** (1986) 3362.
19. J. G. SIMMONS, "Hand Book of Thinfilm Technology", edited by L. I. Maissel and R. Glang (McGraw-Hill, New York, 1970).
20. V. BRAATZ and D. ZAPPE, *Phys. Status Solidi (a)* **86** (1984) 407.
21. J. G. SIMMONS, G. S. NADKARNI and M. C. LANCASTER, *J. Appl. Phys.* **41** (1970) 538.
22. G. S. NADKARNI and J. G. SIMMONS, *ibid.* **41** (1970) 545.
23. D. R. LAMB, "Electrical Conduction Mechanisms in Thin Insulating Films" (Methuen, London, 1967).
24. J. R. YEARGAN and H. L. TAYLOR, *J. Appl. Phys.* **39** (1968) 5600.
25. G. LENGYEL, *ibid.* **37** (1966) 807.
26. J. G. SIMMONS, *Phys. Rev.* **155** (1967) 657.
27. VVR N. RAO, T. S. RAO and N. N. DAS, *J. Phys. Chem. Solids* **47** (1986) 33.
28. RIYAD N. AHMAD-BITAR, M. M. ABDUL-GADER, A. M. ZHILIF and A. M. Y. JABER, *J. Electroanal. Chem.* **143** (1983) 121.
29. M. M. ABDUL-GADER, K. A. WISHAH, Y. A. MAHMUD, M. AL-HAJ ABDALLAH and R. N. AHMAD-BITAR, *Appl. Phys. A* **42** (1987) 3353.
30. K. S. COLE and R. H. COLE, *J. Chem. Phys.* **9** (1941) 341.
31. N. F. MOTT and E. A. DAVIES, "Electronic Processes in noncrystalline Materials", 2nd Edn (Clarendon Press, Oxford, 1979).
32. P. NAGELS, in "Amorphous Semiconductors", edited by M. H. Brodsky (Springer-Verlag, Berlin, Heidelberg, New York, 1973) p. 113.

Received 13 August
and accepted 23 September 1986